Archives of Materials Science and Engineering

Volume 103
Issue 2
June 2020
Pages 49-61

International Scientific Journal
published monthly by the
World Academy of Materials
and Manufacturing Engineering

DOI: 10.5604/01.3001.0014.3354

Estimation of the depth of penetration in a plunging hollow jet using artificial intelligence techniques

D. Bodana [a,*], N.K. Tiwari [a], S. Ranjan [a], U. Ghanekar [b]

[a] Department of Civil Engineering, National Institute of Technology Kurukshetra, India
[b] Department of Electronics and Communication Engineering,
National Institute of Technology Kurukshetra, India
* Corresponding e-mail address: dikshant.bodana@gmail.com
ORCID identifier: https://orcid.org/0000-0002-2529-3984 (U.G.)

ABSTRACT

Purpose: Experimental investigations assessment and comparison of different classical models and machine learning models employed with Gaussian process regression (GPR) and artificial neural network (ANN) in the estimation of the depth of penetration (Hp) of plunging hollow jets.

Design/methodology/approach: In this analysis, a set of data of 72 observations is derived from laboratory tests of plunging hollow jets which impinges into the water pool of tank. The jets parameters like jet length, discharge per unit water depth and volumetric oxygen transfer coefficient (Kla_{20}) are varied corresponding to the depth of penetration (Hp) are estimated. The digital image processing techniques is used to estimate the depth of penetration. The Multiple nonlinear regression is used to establish an empirical relation representing the depth of penetration in terms of jet parameters of the plunging hollow jets which is further compared with the classical equations used in the previous research. The efficiency of MNLR and classical models is compared with the machine learning models (ANN and GPR). Models generated from the training data set (48 observations) are validated on the testing data set (24 observations) for the efficiency comparison. Sensitivity assessment is carried out to evaluate the impact of jet variables on the depth of penetration of the plunging hollow jet.

Findings: The experimental performance of machine learning models is far better than classical models however, MNLR for predicting the depth of penetration of the hollow jets. Jet length is the most influential jet variable which affects the Hp.

Research limitations/implications: The outcomes of the models efficiency are based on actual laboratory conditions and the evaluation capability of the regression models may vary beyond the availability of the existing data range.

Practical implications: The depth of penetration of plunging hollow jets can be used in the industries as well as in environmental situations like pouring and filling containers with liquids (e.g. molten glass, molten plastics, molten metals, paints etc.), chemical and floatation process, wastewater treatment processes and gas absorption in gas liquid reactors.

Originality/value: The comprehensive analyses of the depth of penetration through the plunging hollow jet using machine learning and classical models is carried out in this study.

In past research, researchers were used the predictive modelling techniques to simulate the depth of penetration for the plunging solid jets only whereas this research simulate the depth of penetration for the plunging hollow jets with different jet variables.

Keywords: Depth of penetration, Plunging hollow jets, Machine learning models, Classical models

Reference to this paper should be given in the following way:

D. Bodana, N.K. Tiwari, S. Ranjan, U. Ghanekar, Estimation of the depth of penetration in a plunging hollow jet using artificial intelligence techniques, Archives of Materials Science and Engineering 103/2 (2020) 49-61. DOI: https://doi.org/10.5604/01.3001.0014.3354

METHODOLOGY OF RESEARCH, ANALYSIS AND MODELLING

1. Introduction

Aeration process finds an essential application in water and wastewater treatment. Different forms of aeration systems for the treatment of wastewater, such as diffusers for submerged aeration devices, mechanical surface aerators for the diffusion of atmospheric oxygen on the sewage water surface. Effluent treatment using biological methods is a well-recognized method where an aeration system delivers oxygen to the wastewater to meet the oxygen needs of micro-organisms to oxidize the organic matter. The concept involved in the aeration is the existence of a large air-water interfacial area resulting in the absorption of atmospheric oxygen from the air, causing massive turbulence in the liquid with the formation of a submerged two-phase region and the oxygen is further circulated by diffusion and convection into the liquid body.

Jet aerators are an effective solution for the treatment of biological liquid waste due to low installation, operating, maintenance costs, and high treatment performance [1,2]. It is designed to plunge into the pool of water that absorbs a significant amount of atmospheric air and produces a vast turbulence region created at the water surface due to its impingement with lower energy consumption resulting in higher oxygen transfer. This process is known as plunging jet aeration.

Many research studies exist concerning the importance of jet variables of plunging jets on water oxygenation efficiency. [1,3,4] investigated the transfer of oxygen from the bubbles under the water surface produced by the impact of the plunging water jet. [5] describe the characteristics of mass transfer of the gas-liquid jet mixer using a down flow jet or an up-flow jet with cylindrical and rectangular tanks. [6] experimented with different circular, elliptical, and rectangular nozzle shapes with rounded ends with a penetration angle of 45°, and results show a higher intake of air and oxygen transfer capacity than other shaped nozzles due to the expansion of a water jet with a lower depth of penetration. [7-9] carried out the study on various shaped nozzles with air holes at different locations and compared for water jet expansion, air entrainment rate, depth of penetration, and efficiency of oxygen transfer. [10.11] carried out research on expansion aerators and hollow jet aerators. The expansion aerator performance was improved by providing a jet spreading disk with an angle of 30° below the expansion outlet, and the expansion aerator achieved a higher value of the overall oxygen transfer factor with disk spreading arrangement. [12] observed that the oxygen transfer efficiency of multiple jets was found to be up to 1.6 times higher than that of a single jet, and the oxygen transfer coefficient was correlated with jet variables and number of jets. [13] analysed the hollow conical jet aerator with an angle of 60°, then with the help of the support vector machines applied to experimental data for the estimation of the volumetric transfer coefficient. [2] investigated the potential of supporting vector machines and Gaussian process regression approaches for modelling the overall volumetric transfer coefficient of multiple plunging jet system and proposed that supporting vector machines approach works well by both empirical relationships and Gaussian process approaches and could be used effectively in oxygen transfer modelling. [14] studied the jet angle effect on plane hollow shaped aerators with different 50°, 60°, and 69° angles and multiple jets with curve shaped aerators. The 60° jet aerator performance was best observed in terms of the oxygen transfer factor and oxygen transfer capacity For the single jet aerator, Kla and the oxygen transfer efficiency were obtained higher than the other two multiple jet devices for a low discharge range only. [15,16] used artificial neural network (ANN) and Gaussian process network (GPN) techniques to model air entrainment rates by plunging jets and comparing these modelling techniques with experimental data and results of multiple linear regression (MLR)/multiple non-linear regression (MNLR) and other equations exist in literature. By conducting sensitivity analysis, the nozzle diameter was found to be the most effective parameter on the volumetric air entrainment rate with water jet variables. [17] proposed two different

models to measure the oxygen transfer rate in turbulent cross-flow for a single plunging jet, and the flow visualization technique is used to investigate the complex behaviour of the two-phase air-water flow.

Depth of penetration

During the air-water entrainment process, the distance from the free surface of the water to the extreme point reached by the bubbles is known as depth of penetration (Hp) of a plunging liquid jet. At an extreme position, bubbles velocity is equal to zero, and the force of buoyancy is maximum. Since the geometry of the plume is not perfectly stable, the average weighted time values of depth of penetration are used.

To estimate the depth of penetration, there are many analytical equations available, based on the laboratory experiments. [18,19]studied that the variables governing the amount of air intake by plunging jets by fluctuating the jet velocity, jet turbulence, and jet diameter in terms of penetration depth. [20] found that the truncated circular nozzles have high efficiency in terms of bubble penetration depth, volumetric air intake, and oxygen transfer and are recommended for practical applications of aeration. [21] investigated that the penetration depth (up to 1.7 m) of the plunging liquid jets at high flow rates, and it was modelled using multivariate non-linear regression and ANN. It was shown to increase with increasing momentum flows and decreasing jet lengths.

The above researchers investigated the depth of penetration for solid jets, which is based on the laboratory experiments. Therefore, to determine the air entrainment in terms of depth of penetration for hollow jets, further investigation is vital.

2. Material and methods

2.1. Hollow jet aeration device

Plunging hollow jet is an aeration device that consists of two components .i.e. discharging pipe and conical disc. A conical disc (60° angle from the base) was fitted at the outlet of the discharging pipe with the help of fasteners; thus, it forms a hollow jet device. This device was installed in the main pipeline, and it was allowed to run. The water flow developed in the jet was emerging out through the annular opening between the discharging pipe and conical disc with high velocity (jet velocity), and it is spread in all the directions uniformly. It absorbs a significant amount of atmospheric air before the plunge into a pool of water. It creates high turbulence region on the water surface as compared to a solid jet. Tapered and Cylindrical hollow jets were the two different jet aerators used in this study (Fig. 1).

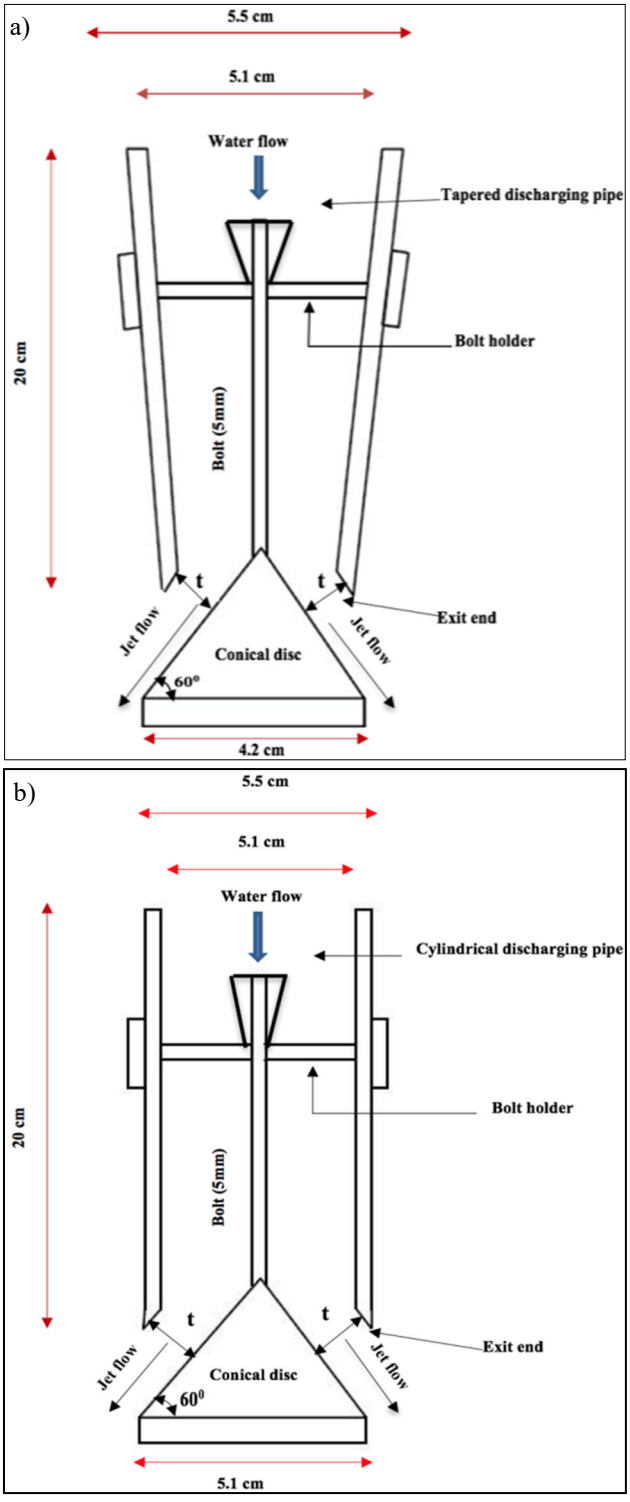

Fig. 1. a) Tapered hollow jet, b) cylindrical hollow jet

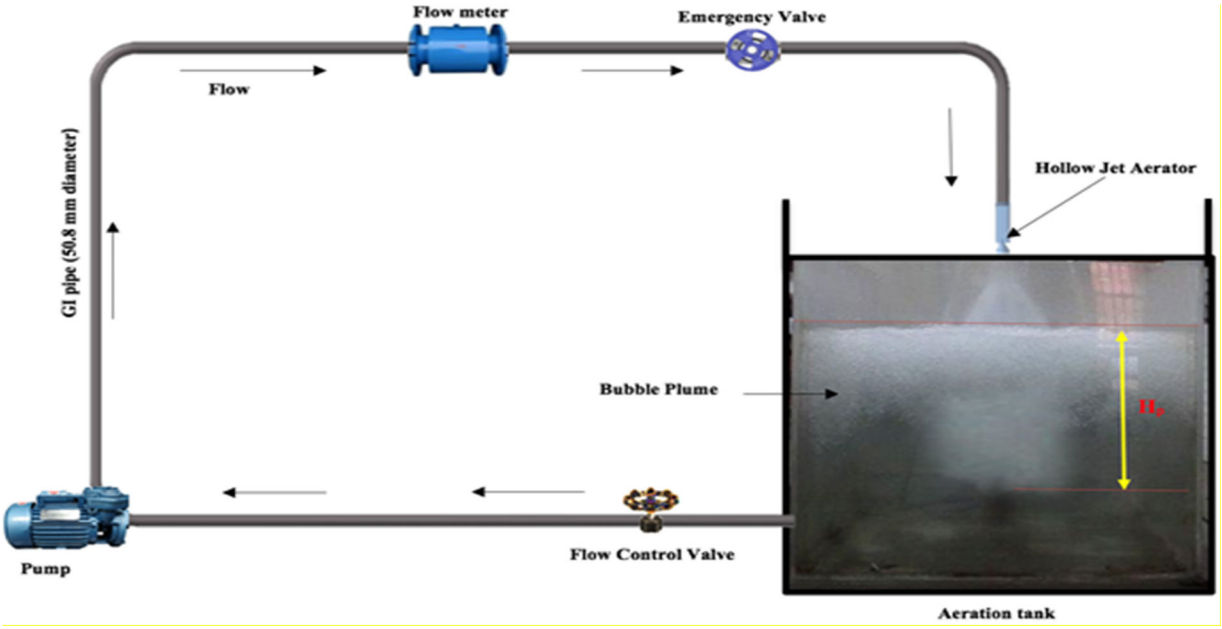

Fig. 2. Layout of experimental setup

2.2. Experimental setup

Experiments were carried out in an aeration tank (Fig. 2) with water carrying capacity (0.87 x 0.87 x 0.87) m^3 attached to a centrifugal water pump of capacity 1 HP using a 2-inch (diameter) galvanised iron pipeline. The tank was fabricated from transparent acrylic sheets. A digital flow meter which was fitted with the galvanized iron pipe used to measure the flow discharge with accuracy of ±0.5% of reading in the pipeline. There are two control valves present in the pipe .i.e. the first valve was used to control the flow of water and the second valve is an emergency valve which was used when the water was choked in the pipe due to some reasons at the time of first valve ceased to operate.

For all the experiments, tap water was used, and the water level in the aeration tank was kept at 0.65 m. At the outlet of the pipe, the hollow jet aeration device was installed for three consecutive jet lengths (distance between the jet and water surface) of 0.1m, 0.2 m, and 0.3 m.

Jet thickness was manually adjusted by the cone, which was fitted in the hollow jet. For a particular hollow jet aerator, a specified volume of water was filled into the tank to obtain the concentration of oxygen transferred int the water. After some time, the initial DO (Co) of water is measured by Azide modification test [22] by taking a sample of water in the BOD bottles and then, run the aerator for the specific period (t= 40 s) and take the dissolved oxygen (DO) present in the initial water is deoxygenated up to 1-2 mg/l by adding a sufficient amount sodium sulphite with the cobalt chloride as a catalyst in the water [13]. samples of final DO (C_t) in the BOD bottles for the DO measurement. During the experiments, the temperature (T) of water recorded to determine the saturated DO (Cs). The experiment was repeated for different observations using different jet aerators, and then estimating the volumetric oxygen transfer coefficient (K_LA) from the given relation

$$(\mathrm{Kla})_T = \frac{1}{t}\mathrm{Ln}\left[\frac{C_s - C_0}{C_s - C_t}\right] \quad (1)$$

The following relationship allows estimation of the volumetric oxygen transfer coefficient at a standard temperature of 20°C and a pressure of 1 atm.

$$\mathrm{Kla}_{20} = (\mathrm{Kla})_T (1.024)^{(20-T)} \quad (2)$$

2.3. Image processing technique

The experimental method for estimating the depth of penetration was generally the same for all the observations. The hollow jet device was installed at the outlet of the pipe, and now, the device is allowed to run. By regulating the control valve, the desired flow rate is adjusted. For the visual analysis of the depth of penetration, a camera was placed in front of the water tank at a distance of 1.5 m, and a LED light illuminates the bubble plume in the water tank. A camera was used to capture the series of images of bubble plume inside the water tank at a rate of 10 images per second, and

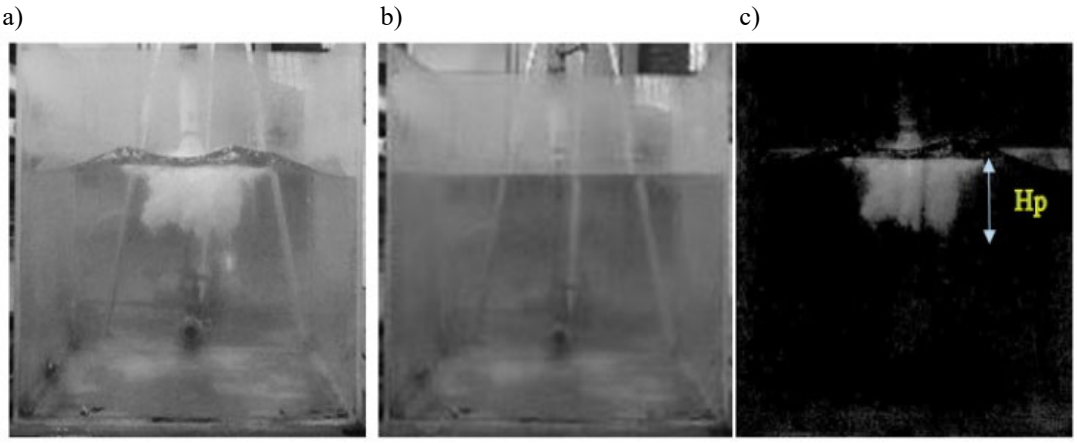

Fig. 3. Image subtraction process: a) final image, b) initial image, c) subtracted image

the resolution of the camera is 24 megapixels. For same experimental condition, two types of images were captured i.e., the first type of images were captured when there is no bubble plume (jet aerator is not allowed to run) in the tank which is known as initial image and the second type of images were captured when the bubble plume exists (jet aerator is allowed to run) in the tank, known as final image. Therefore, the subtraction of the initial image from the final image is known as the subtracted image (Fig. 3). Subtracted image contains only bubble plume. Now, the depth of bubble plume estimated in terms of pixels that were further converted to the SI unit. The depth of bubble plume is known as the depth of penetration. Now, the experiment was repeated for different jet lengths.

2.4. Machine learning techniques

Artificial neural network (ANN)

ANN is an information processing system that has been developed as a generalization of the mathematical model of human cognition. A neural network is a network of inter-connected neurons, inspired by human brains. The function of a neural network is to generate the output pattern (results) when presented with an input pattern. It is a machine learning model used for numerical prediction [23-25]. The multi-layer perceptron (MLP) is among the most widely used ANNs in several fields of research. This analysis uses MLP with a three-layer computing network consisting of an input layer, a hidden layer, and an output layer. The hidden layer that exists between the layers of input and output includes the components of processing called neurons. The input layer accepts values from the input parameters, and the output layer gives an estimate. The hidden layers and nodes perform an essential role in the successful implementation of the neural network. Figure 4 showed the ANN structure in which three input variables were used as jet length (Lj), discharge per unit depth (q), and volumetric oxygen transfer coefficient, whereas the depth of penetration was the output variable.

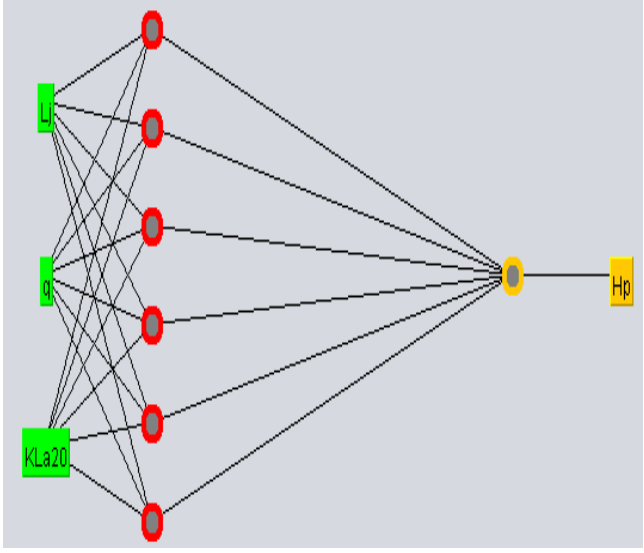

Fig. 4. ANN structure

Gaussian process regression (GPR)

GPR is the most advanced Bayesian technique for classification and regression studies. When the variance and correlation function is selected, the most elegant grouping of hyperparameters can be calculated by unravelling the maximum likelihood of the computational problem [26]. The result of the GPR model has a precise probabilistic analysis, which provides a measure of the uncertainty

estimation. GPR was used to predict the transfer of oxygen [27,28], the modelling of infiltration by GPR [29].The GPR based kernels used in this study are:

1. GP-Normalised Polyfunction kernel (NORMPOLY):

$$K(x_j, x_k) = K(x_j, x_k)/\sqrt{K(x_j, x_j), K(x_k, x_k)} \quad (3)$$

2. GP- Pearson VII function kernel (PUK):

$$K(x_j, x_k) = 1/\left[1 + \left(2\sqrt{\|x_j - x_k\|^2}\sqrt{2^{(1/\omega)} - 1}/\sigma\right)^2\right]^{\omega} \quad (4)$$

3. GP-Radial Basis function kernel (RBF):

$$K(x_j, x_k) = e^{-\gamma|x_j - x_k|^2} \quad (5)$$

4. GP-Polynomial function kernel (POLYK):

$$K(x_j, x_k) = \{(x_j, x_k) + 1\}^d \quad (6)$$

These kernels were used to predict the performance of depth of penetration (Hp) in terms of CC and RMSE, which is depending on kernel attributes (γ, ω, σ, d). The computation of user defined attributes is carried out by performing multiple runs on the training data and examining the efficiency of the established models on the testing data. The flow chart of modelling techniques in shown in Figure 5.

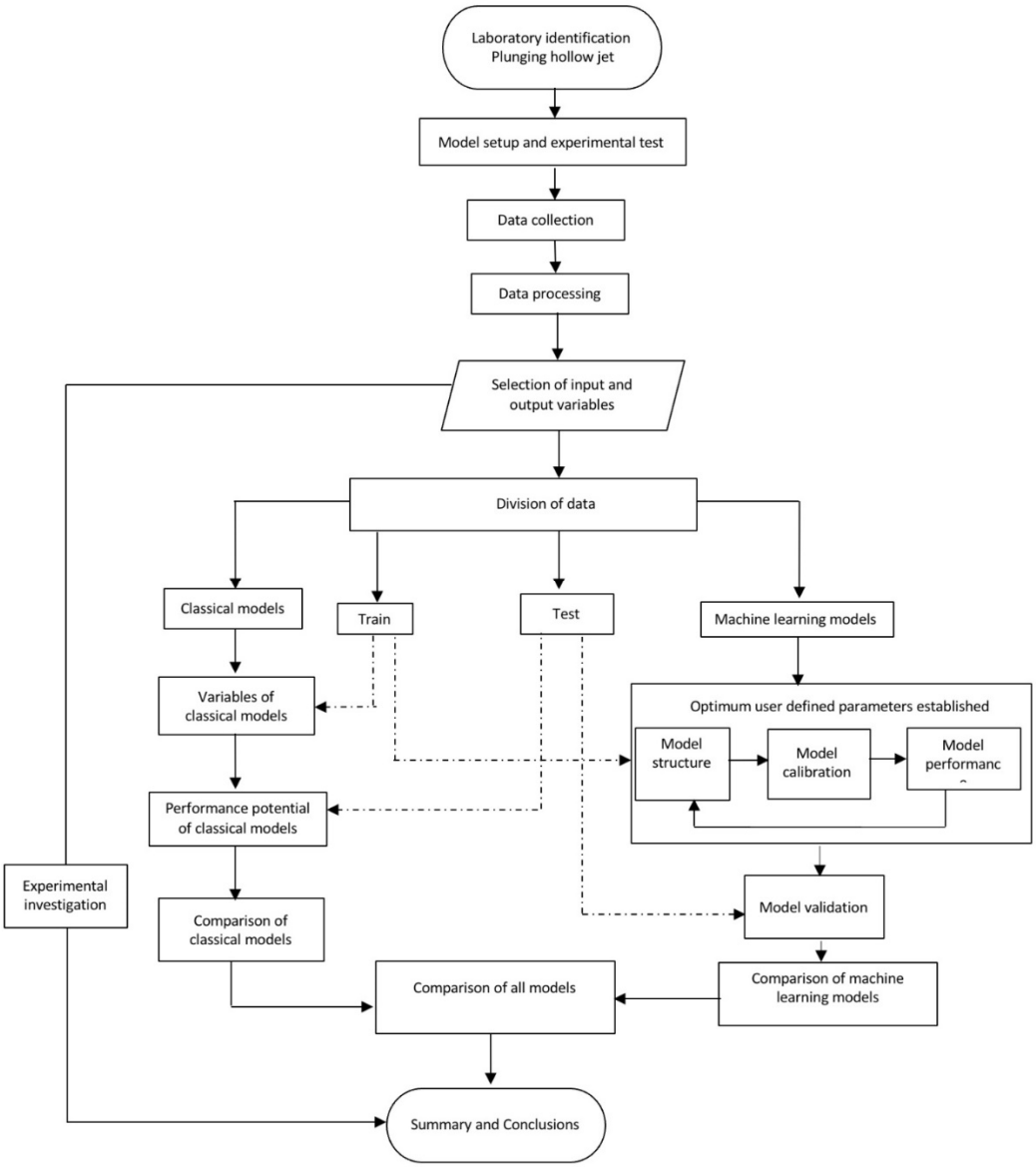

Fig. 5. Flow chart of modelling techniques

2.5. Multi non-linear regression (MNLR)

A multi-nonlinear relation is defined by using depth of penetration (Hp) as dependable parameter whereas the jet length (L_j), discharge per unit water depth (q), and volumetric oxygen transfer coefficient (Kla_{20}) is considered as explanatory parameter. A MNLR model is developed from training data that express the 'Hp' in the form of jet variables (L_j, q and KLa_{20}) from the following relationship

$$Hp = f(\alpha L_j^{y_1}\, q^{y_2}\, Kla_{20}^{y_3}) \quad (7)$$

Where α is the constant, y_1, y_2, y_3 are the function coefficients and can be obtained by reducing the amount of error squares in approximation.

$$Hp = 10.23\, L_j^{-0.325} q^{1.047} Kla_{20}^{-0.2} \quad (8)$$

2.6. Data sets

For the analysis of machine learning models and classical models, the dataset was prepared, which consists of 72 observations. Out of this 72 observation, the total number of observations used for the training data was 48, while the remaining 24 were selected to test the model. The input parameters consist of jet length (Lj), discharge per unit depth (q), KLa_{20}, while the depth of penetration (Hp) was considered to be the output. The data categorization of testing and training was based on arbitrary selection. The attributes of the dataset is given in the Table 1.

3. Results and discussion

3.1. Experimental analysis

The performance of tapered and cylindrical hollow jets was shown in Figures 6 and 7. In tapered hollow jet, the outlet area was intentionally reduced, which increases the efficiency of the jet in terms of Hp and Kla_{20}, whereas in the cylindrical section, the inlet and outlet area was the same, and the efficiency is slightly lesser than the tapered hollow jet. There is a linear variation between penetration depth (Hp), and discharge per unit depth (q) for the different jet lengths 10 cm, 20 cm, and 30 cm through the tapered and cylindrical hollow jets were shown in the Figure 6.

Table 1.
Range of attributes dataset for the preparation of model

Stage	Range	L_j	q	Kla_{20}	H_p
Total data set	Minimum	0.100	0.003	0.002	0.099
	Maximum	0.300	0.010	0.037	0.386
	Mean	0.200	0.007	0.014	0.237
	STD	0.082	0.002	0.009	0.067
	Kurtosis	-1.521	-1.393	-0.723	-0.714
	Skewness	0.000	-0.140	0.573	-0.080
Training data set	Minimum	0.100	0.003	0.002	0.099
	Maximum	0.300	0.010	0.037	0.386
	Mean	0.200	0.007	0.013	0.238
	STD	0.083	0.002	0.009	0.070
	Kurtosis	-1.533	-1.156	-0.441	-0.679
	Skewness	0.000	-0.197	0.664	-0.059
Testing data set	Minimum	0.100	0.005	0.003	0.122
	Maximum	0.300	0.009	0.033	0.343
	Mean	0.200	0.007	0.014	0.237
	STD	0.083	0.002	0.009	0.062
	Kurtosis	-1.568	-2.190	-1.247	-0.890
	Skewness	0.000	0.000	0.420	-0.158

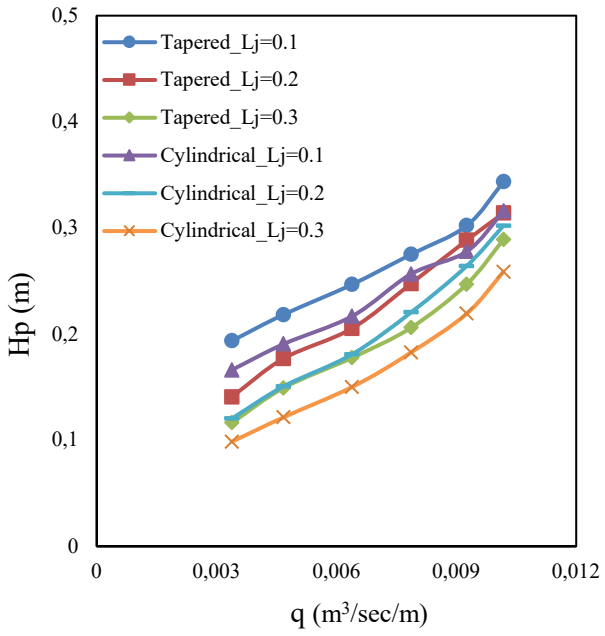

Fig. 6.Variation between q and Hp Lj = 0.1, 0.2, 0.3 m for tapered and cylindrical hollow jet

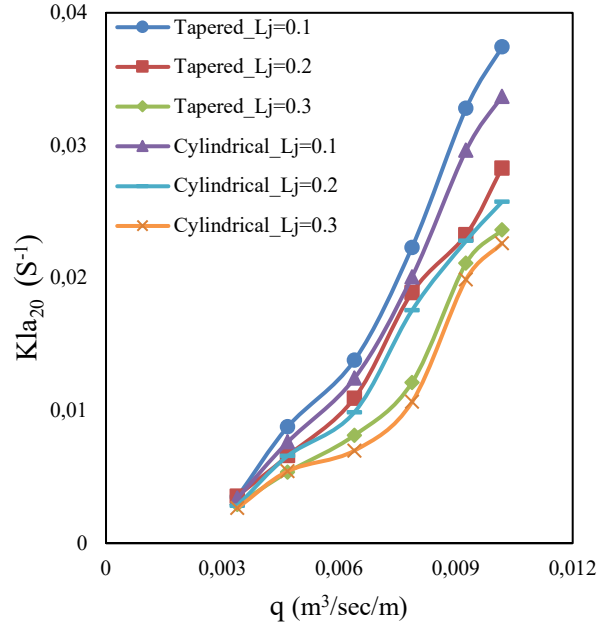

Fig. 7. Variation between q and Kla_{20} at Lj = 0.1, 0.2, 0.3 m for tapered and cylindrical hollow jet

With the decrease in jet length, it was observed that the depth of penetration (Hp) increases vertically with the increase in discharge per unit depth, it means that the depth of penetration is directly proportional to the discharge per unit depth and inversely proportional to the jet length. Due to the increase in discharge per unit depth, the jet impact on the pool surface of water increases, which creates intense turbulence andbhigh shear in the water. Therefore,it increases the oxygenation of pool water. The oxygenation was measured in terms of Kla, and further, it was converted to Kla_{20}. The plot between the Kla_{20} and discharge per unit depth was shown in the Figure 7. The results of tapered hollow jets were slightly better than the cylindrical hollow jets.

3.2. Results of classical models

A comparison between the actual penetration depth and the predicted penetration depth for the defined test and train data set is shown in Figures 8 and 9, which were used to develop the classical models (Tabs. 2 and 3) and it was found that the outcomes of the defined test and train values of MNLR were far away from the perfect agreement line. Still, the CC value (0.9) of MNLR was very high, and the RMSE value (0.027) of MNLR was very low.

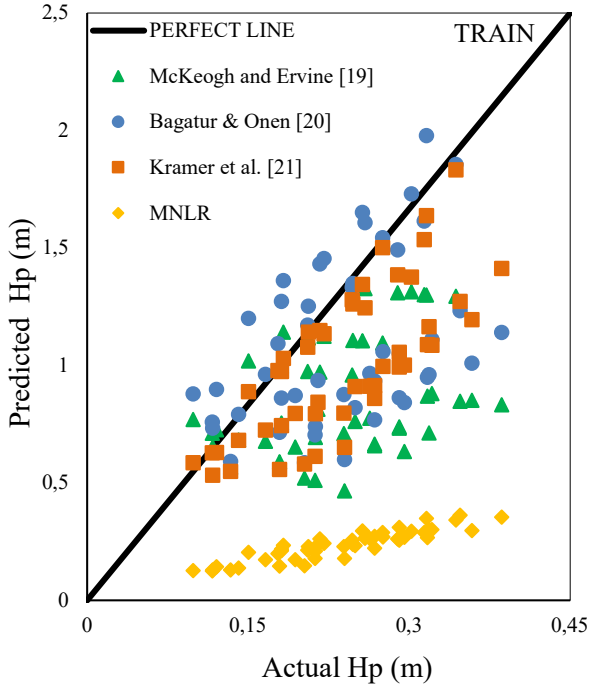

Fig. 8. Scattering of Hp using classical models for training data

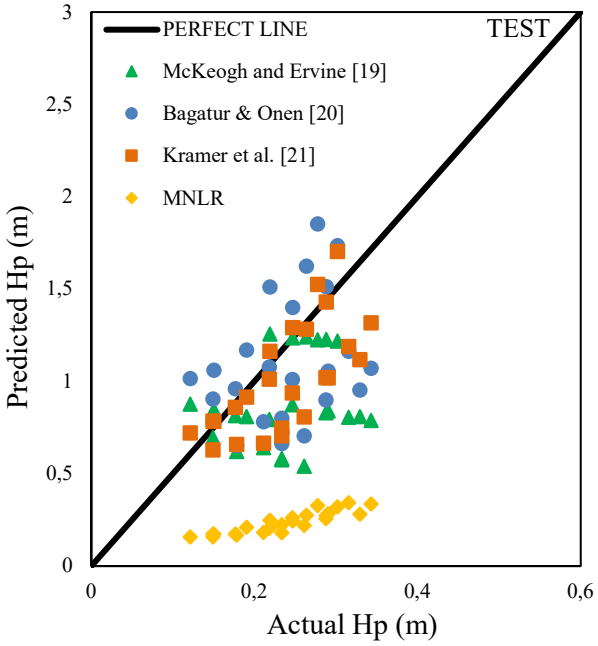

Fig. 9. Scattering of Hp using classical models for testing data

The performance of other classical models like [19-21] was not better than the MNLR model. But the [21] model was comparable better than the [19,20] in terms of CC and RMSE. The classical models show poor prediction efficiency to evaluate the depth of penetration (Hp) except MNLR model. The classical equations were given in Table 2.

Table 2.
Classical equations

Model	Equation	No.
McKeogh and Ervine	$H_P = 2.6\left(V_j d_o\right)^{0.7}$	(9)
Bagatur and Onen	$H_P = 4.84\, V_j^{0.73}\, d_0^{\,0.93}\, L_j^{-0.21} (\sin\theta)^{0.73}$	(10)
Kramer et al.	$H_P = 0.2\,(\rho Q V_j)^{0.39}\, L_j^{-0.26}$	(11)
MNLR	$Hp = 10.23\;\; L_j^{-0.325}\, q^{\,1.047}\, Kla_{20}^{-0.2}$	(12)

3.3. Results of modelling technique

In the Figures 10 and 11, it is shown that the different machine learning models were generated for specific sets of testing and training data. ANN and GPR are the two types of machine learning techniques were used in this study, in which the GPR model is sub-categorized into four types – RBFK, POLYK, PUK, and Normalised POLYK. To develop the ANN model, a systematic approach of hit and trial was to be done for the iterative parameters like learning rate, hidden layers, momentum, and learning rate. ANN model contains the learning rate=0.1, hidden layers = 6, momentum rate =0.3 and training time = 5000. The CC and RMSE values of the ANN model for the testing data are 0.9322 and 0.0224 (Figs. 12 and 13), which is less than the GPR models.

Table 3.
Efficiency of models

Models	Training Data		Testing Data	
	CC	RMSE	CC	RMSE
Machine learning methods				
ANN	0.9434	0.0248	0.9322	0.0224
GP_RBFK	0.9484	0.0221	0.9371	0.0231
GP_POLYK	0.9535	0.0179	0.9331	0.0324
GP_PUK	0.9480	0.0222	0.9370	0.0230
GP_NORMPOLYK	0.9467	0.0225	0.9293	0.0252
Classical methods				
Bagatur & Onen	0.4263	0.9174	0.3483	0.9171
Kramer et al.	0.7460	0.8141	0.7008	0.8142
McKeogh and Ervine	0.3306	0.6731	0.2447	0.6735
MNLR	0.9094	0.0290	0.9003	0.0268

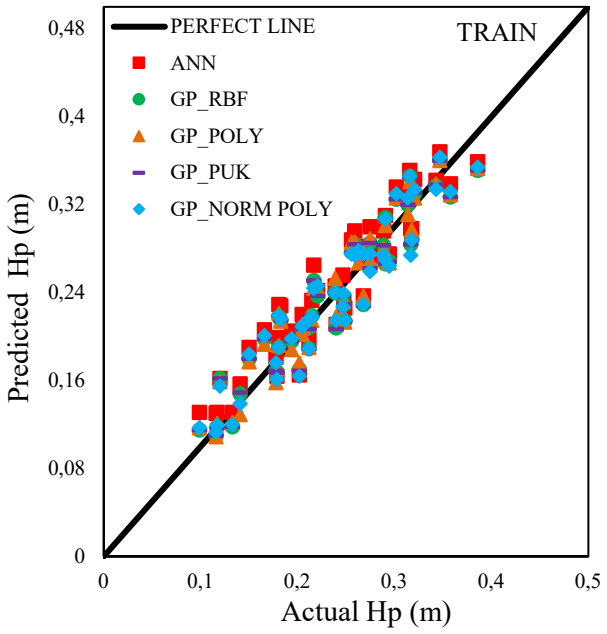

Fig. 10. Scattering of Hp using machine learning models for training data

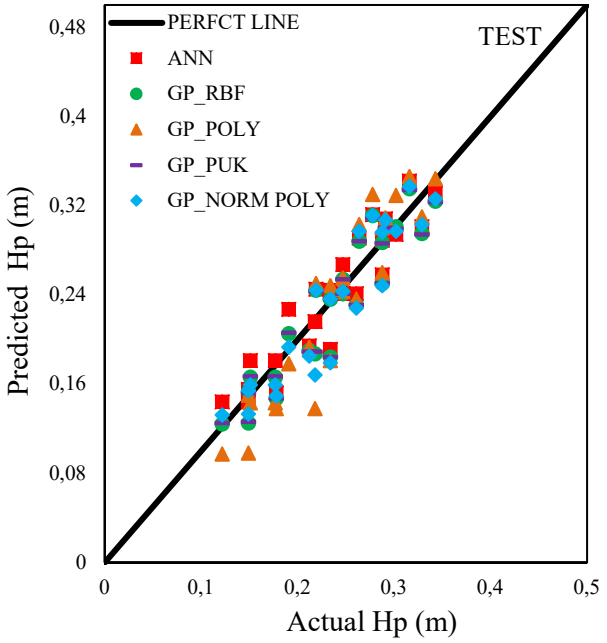

Fig. 11. Scattering of Hp using machine learning models for testing data

Similarly, GPR models were developed for the same set of test and train data which was previously used by the ANN model. The performance of RBFK (Gamma = 0.03 and Noise = 0.001) and PUK (Sigma = 11, Omega = 8, and Noise = 0.001) was slightly better than the POLYK and Normalised POLYK models in terms of CC and RMSE. The CC and RMSE value of RBFK and PUK was almost same (Tab. 3), which is equal to 0.937 and 0.023 (test data). The results of POLYK (Exponent = 0.3 and Noise = 0.001) and Normalised POLYK (Exponent = 2 and Noise = 0.001) models were satisfactory, but however, it was not better than the RBFK and PUK models.

Overall review of Figures 12 and 13 reveals that the precision of the ANN model for estimating the depth of penetration was slightly lower than that of the GP-based models except for normalized POLYK model, so it is better to predict the depth of penetration from the GP based models rather than ANN models.

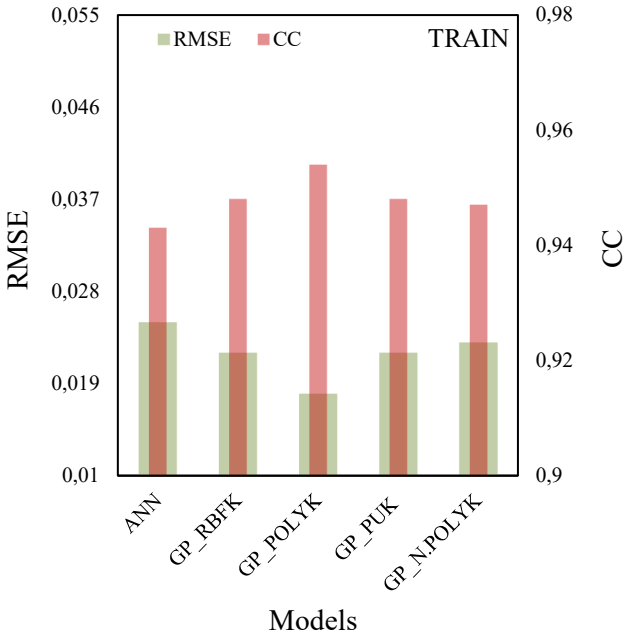

Fig. 12. Performance of Machine learning models for predicting the Hp for training data

3.4. Comparison of models

In classical models, the MNLR model has better estimation efficiency than the other classical models [19-21]. From the Table 3, it was observed that the performance of machine learning models for the given testing and training dataset was much better than the classical models in the prediction of Hp. However, RBF and PUK model based on GP regression has high efficiency to predict the Hp with the high value of CC = 0.937 and the least value of RMSE = 0.023 than the other applied models. The results of other machine learning models were satisfactory but it was slightly less than the RBF and PUK model.

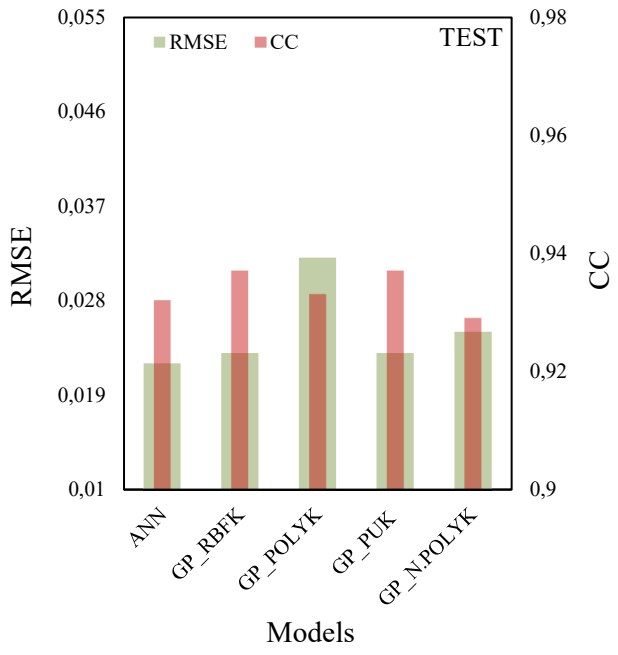

Fig. 13. Performance of machine learning models for predicting the Hp for testing data

The ranking of models in order to estimate the depth of penetration (Hp) were likely to be as GP_RBF (1st), GP_PUK (2nd), GP_POLYK (3rd), ANN (4th), GP_NORMPOLYK (5th), MNLR (6th), Kramer et al. [21] (7th), Bagatur & Onen [20] (8th) and McKeogh and Ervine [19] (9th). [19,20] were shows very poor results as compare to other models. [21] was also gives poor results in comparison to other models but it is far better than the [19,20]. Therefore, the best models which predict the depth of penetration of bubble plume entrained by the plunging hollow jets are GP_RBFK and GP_PUK

3.5. Sensitivity analysis

The most influential jet variable which affects the depth of penetration through hollow jet was determined by the sensitivity analysis. In machine learning models, the performance of GP regression based RBF and PUK kernels was better than the other regression models. A specific set of test and train data was generated by removing a single jet variable input simultaneously. The outcomes were presented in terms of coefficient of correlation (CC) and the root mean square error (RMSE). The extent of variation in CC and RMSE values indicates the influence of jet variable on the depth of penetration.

It was observed that the jet length (Lj) was the most influential jet variable, and have a vital role in the estimation of the depth of penetration as compared to other jet variables. Relative fluctuations in CC and RMSE by eliminating the jet length were significantly higher (Tab. 4).

Table 4.
Sensitivity of models

Model	Absent	Input	Output	CC	RMSE
Training Data					
GP_RBFK	-	Lj, q, Kla_{20}	Hp	0.9484	0.0221
	Lj	q, Kla20	Hp	0.8607	0.0353
	q	Lj, Kla20	Hp	0.8992	0.0305
	Kla20	Lj, q,	Hp	0.9329	0.0206
GP_PUK	-	Lj, q, Kla_{20}	Hp	0.9480	0.0222
	Lj	q, Kla20	Hp	0.8603	0.0355
	q	Lj, Kla20	Hp	0.8999	0.0305
	Kla20	Lj, q,	Hp	0.9329	0.0206
Testing Data					
GP_RBFK	-	Lj, q, Kla_{20}	Hp	0.9371	0.0231
	Lj	q, Kla20	Hp	0.8096	0.0361
	q	Lj, Kla20	Hp	0.8617	0.0326
	Kla20	Lj, q,	Hp	0.9094	0.0259
GP_PUK	-	Lj, q, Kla_{20}	Hp	0.9370	0.0230
	Lj	q, Kla20	Hp	0.8095	0.0361
	q	Lj, Kla20	Hp	0.8616	0.0326
	Kla20	Lj, q	Hp	0.9094	0.026

4. Conclusions

Estimation of volumetric oxygen transfer coefficient (KLa_{20}) and depth of penetration of bubbles entrained by plunging hollow jet has been determined in the 0.87 m long and 0.87 m wide aeration tank at different flow rates (ranges: 2-6 L/S) with jet lengths of 10, 20, and 30 cm. However, these data-driven models mentioned in the research may assist the professionals and experts to estimate depth of penetration and KLa_{20}.

The depth of penetration and volumetric oxygen transfer coefficient KLa_{20} for the plunging hollow water jet increased with the increase in discharge per unit depth and decreased with the reduction of jet length**.** The performance of the tapered hollow jet was slightly better than the cylindrical hollow jets in terms of Hp and KLa_{20}.

In classical models, The results of MNLR (CC=0.900, and RMSE=0.027) developed by input variables (jet length, discharge per unit water depth, and Kla_{20}) was remarkably better than the other classical models like Bagatur & Onen (2014), Kramer et al. (2016) and McKeogh and Ervine (1981). In machine learning models, The performance of GP based RBFK and PUK models was slightly better than the other GP based models (POLYK and Normalized POLYK) and ANN model. The CC and RMSE values of RBFK and PUK models were same, which is equal to 0.937 and 0.023.

The machine learning models were far better than the classical models except MNLR model. The CC and RMSE values of MNLR model are slightly lesser than the machine learning models but it was satisfactory. The results of sensitivity analyses show that the jet length is the most crucial jet variable which affects the depth of penetration.

References

[1] E. van de Sande, J.M. Smith, Mass transfer from plunging water jets, The Chemical Engineering Journal 10/3 (1975) 225-233. DOI: https://doi.org/10.1016/0300-9467(75)88040-3

[2] S. Deswal, Modeling oxygen-transfer by multiple plunging jets using support vector machines and Gaussian process regression techniques, International Journal of Civil and Environmental Engineering 5/1 (2011) 1-6.

[3] X.L. Qu, L. Khezzar, D. Danciu, M. Labois, D. Lakehal, Characterization of plunging liquid jets: A combined experimental and numerical investigation, International Journal of Multiphase Flow 37/7 (2011) 722-731. DOI: https://doi.org/10.1016/j.ijmultiphaseflow.2011.02.006

[4] K. Harby, S. Chiva, J.L. Muñoz-Cobo, An experimental study on bubble entrainment and flow characteristics of vertical plunging water jets. Experimental Thermal and Fluid Science 57 (2014) 207-220. DOI: https://doi.org/10.1016/j.expthermflusci.2014.04.004

[5] K. Tojo, K. Miyanami, Oxygen transfer in jet mixers, The Chemical Engineering Journal 24/1 (1982) 89-97. DOI: https://doi.org/10.1016/0300-9467(82)80054-3

[6] T. Bagatur, A. Baylar, N. Sekerdag, The effect of nozzle type on air entrainment by plunging water jets, Water Quality Research Journal 37/3 (2002) 599-612. DOI: https://doi.org/10.2166/wqrj.2002.040

[7] A. Ohkawa, D. Kusabiraki, Y. Shiokawa, N. Sakai, M. Fujii, Flow and oxygen transfer in a plunging water jet system using inclined short nozzles and performance characteristics of its system in aerobic treatment of wastewater, Biotechnology and Bioengineering 28/12 (1986) 1845-1856. DOI: https://doi.org/10.1002/bit.260281212

[8] A. Baylar, M.E. Emiroglu, Air entrainment and oxygen transfer in a venturi, Proceedings of the Institution of Civil Engineers – Water and Maritime Engineering 156/3 (2003) 249-255. DOI: https://doi.org/10.1680/wame.2003.156.3.249

[9] M.E. Emiroglu, A. Baylar, Role of nozzles with air holes in air entrainment by a water jet, Water Quality Research Journal 38/4 (2003) 785-95. DOI: https://doi.org/10.2166/wqrj.2003.049

[10] S. Ranjan, Hydraulics of hollow jet aerators. Journal of Indian Water Resources Society 27/1-2 (2007) 27-31.

[11] S. Ranjan, Hydraulics of jet aerators, Journal of the Institution of Engineers (India): Environmental Engineering Division 88 (2008) 29-32.

[12] S. Deswal, D.V. Verma, Air-water oxygen transfer with multiple plunging jets, Water Quality Research Journal 42/4 (2007) 295-302. DOI: https://doi.org/10.2166/wqrj.2007.031

[13] S. Deswal, D.V. Verma, Performance evaluation and modeling of a conical plunging jet aerator, International Journal of Mathematical, Physical and Engineering Sciences 2/1 (2008) 33-37.

[14] M. Kumar, S. Ranjan, N.K. Tiwari, R. Gupta, Plunging hollow jet aerators-oxygen transfer and modelling, ISH Journal of Hydraulic Engineering 24/1 (2018) 61-67. DOI: https://doi.org/10.1080/09715010.2017.1348264

[15] T. Bagatur, F. Onen, A predictive model on air entrainment by plunging water jets using GEP and ANN, KSCE Journal of Civil Engineering 18/1 (2014) 304-314. DOI: https://doi.org/10.1007/s12205-013-0210-7

[16] F. Onen, Prediction of penetration depth in a plunging water jet using soft computing approaches, Neural Computing and Applications 25/1 (2014) 217-127. DOI: https://doi.org/10.1007/s00521-013-1475-y

[17] M.E. Jahromi, M. Khiadani, Experimental study on oxygen transfer capacity of water jets discharging into turbulent cross flow, Journal of Environmental Engineering 143/6 (2017) 04017007. DOI: https://doi.org/10.1061/(ASCE)EE.1943-7870.0001194
[18] C. Clanet, J.C. Lasheras, Depth of penetration of bubbles entrained by a plunging water jet, Physics of Fluids 9/7 (1997) 1864-1866. DOI: https://doi.org/10.1063/1.869336
[19] E.J. McKeogh, D.A. Ervine, Air entrainment rate and diffusion pattern of plunging liquid jets, Chemical Engineering Science 36/7 (1981) 1161-1172. DOI: https://doi.org/10.1016/0009-2509(81)85064-6
[20] T. Bagatur, Experimental analysis of flow characteristics from different circular nozzles at plunging water jets, Arabian Journal for Science and Engineering 39/4 (2014) 2707-2719. DOI: https://doi.org/10.1007/s13369-014-0967-0
[21] M. Kramer, S. Wieprecht, K. Terheiden, Penetration depth of plunging liquid jets – A data driven modelling approach, Experimental Thermal and Fluid Science 76 (2016) 109-117. DOI: https://doi.org/10.1016/j.expthermflusci.2016.03.007
[22] A.D. Eaton, L.S. Clesceri, M.A.H. Franson, E.W. Rice, A.E. Greenberg (eds.), Standard Methods for Examination of Water And Wastewater, 21th Edition, American Public Health Association, New York: 2005.
[23] N.K. Tiwari, Evaluating hydraulic jump oxygen aeration by experimental observations and data driven techniques, ISH Journal of Hydraulic Engineering (2019) 1-5 (published online). DOI: https://doi.org/10.1080/09715010.2019.1658551
[24] N.K. Tiwari, P. Sihag, Prediction of oxygen transfer at modified Parshall flumes using regression models, ISH Journal of Hydraulic Engineering 26/2 (2020) 209-220. DOI: https://doi.org/10.1080/09715010.2018.1473058
[25] N.K. Tiwari, P. Sihag, D. Das, Performance evaluation of tunnel type sediment excluder efficiency by machine learning, ISH Journal of Hydraulic Engineering (2019) 1-3 (published online). DOI: https://doi.org/10.1080/09715010.2019.1667883
[26] C.E. Rasmussen, Gaussian processes in machine learning, in: O. Bousquet, U. von Luxburg, G. Rätsch (eds.), Advanced Lectures on Machine Learning, ML 2003. Lecture Notes in Computer Science, vol. 3176, Springer, Berlin, Heidelberg, 2004, 63-71. DOI: https://doi.org/10.1007/978-3-540-28650-9_4
[27] M. Kumar, N.K. Tiwari, S. Ranjan, Prediction of oxygen mass transfer of plunging hollow jets using regression models, ISH Journal of Hydraulic Engineering 26/1 (2020) 23-30. DOI: https://doi.org/10.1080/09715010.2018.1435311
[28] M. Kumar, N.K. Tiwari, S. Ranjan, Kernel function based regression approaches for estimating the oxygen transfer performance of plunging hollow jet aerator, Journal of Achievements in Materials and Manufacturing Engineering 95/2 (2019) 74-84. DOI: http://doi.org/10.5604/01.3001.0013.7917
[29] P. Sihag, B. Singh, A. Sepah Vand, V. Mehdipour, Modeling the infiltration process with soft computing techniques, ISH Journal of Hydraulic Engineering 26/2 (2020) 138-152. DOI: https://doi.org/10.1080/09715010.2018.1464408